ChemPubSoc Europe

DOI: 10.1002/chem.201403721

CHEMISTRY A European Journal Full Paper

Supramolecular Chemistry

Controlling the Size and Morphology of Supramolecular Assemblies of Viologen–Resorcin[4]arene Cavitands

Ruslan R. Kashapov,* Sergey V. Kharlamov, Elza D. Sultanova, Rezeda K. Mukhitova, Yuliana R. Kudryashova, Lucia Y. Zakharova, Albina Y. Ziganshina, and Alexander I. Konovalov[a]

Abstract: A novel class of self-assembling nanoparticles is formed with viologen–resorcin[4]arene cavitands; the association model is strongly controlled by their hydrophobicity. Interestingly, the cavitand assemblies are designed through click chemistry to form self-assembled noncovalently connected aggregates through counterion displacement. The iodide and benzoate ions are utilized as strongly polarizable counterions to induce cavitand self-assembly. The counterion-mediated decrease in hydrophilicity of the viologen–resorcin[4]arenes is the underlying trigger to induce particle formation. These particles can be used as nanocontainers and find their applications in delivery systems.

Introduction

Control of molecular self-assembly is an important goal of modern science.[1] A growing interest in the self-assembly processes is caused primarily by the fabrication of micro- and nanoscale structures for various molecular device applications.[2] Self-assembly inducing the formation of different supramolecular assemblies has been widely explored as a kind of facilitated nanocontainer. The success of this application requires the development of versatile mechanisms of self-assembly to produce nanocontainers with controlled functions and structures.[3] There are several strategies for their creation and, alternatively, the nanocontainer structure can be achieved through the self-assembly of macrocyclic platforms.[4] Within the latter methodology, the calix[4]arene platform has demonstrated its potential for building up these systems.

Water-soluble amphiphilic calixarenes consist of hydrophobic and -philic blocks connected with aromatic rings. They are interesting for applications because they may combine the properties of surfactants and macromolecules. Similar to low-molecular-weight surfactants, these macrocycles self-assemble in aqueous solutions to form various types of assemblies[5–10] that may be used for molecular encapsulation. In addition, there are studies demonstrating the effects of additives such as solvents on the self-assembling properties of uncharged macrocycles.[11–15]

Many calix[4]arene-[6,16–23] and calix[4]resorcinarene-based[9–15,17,18,24] nanocontainers have been reported. Calix[4]arenes and calix[4]resorcinarenes contain concave surfaces available for guest inclusion; however, they are generally less predictable during self-assembly due to relatively flexible framework. The flexible molecules often need guest molecules to act as templates to form discrete structures. The relative rigidity of the resorcin[4]arene skeleton apparently decreases steric strain or ion repulsion and enhances binding of guests relative to that of calix[4]arene. Moreover, the position of a crown ether linkage between neighboring phenyl rings instead of the hydroxyl groups increases the hydrophobicity of resorcin[4]arene and improves the stability of the nanoparticles formed by these molecules in water. Therefore, herein, the resorcin[4]arene-based nanocontainers were prepared in aqueous solutions for the first time.

To generate novel resorcin[4]arene-based nanocontainers, water-soluble resorcin[4]arene cavitands consisting of four viologen units on the upper rim of resorcin[4]arene platform were chosen. Viologen moieties attached to a macrocyclic platform confer water solubility to calixarenes with high hydrophobicity. Moreover, linking of viologen with the macrocyclic platform enables a compound to be obtained with a multiply charged cation and a well-organized structure, in which the electron-acceptor properties can be controlled. Previously, we showed that viologen–resorcin[4]arenes (VRs) with different tail lengths on the lower rim (Scheme 1) exhibited acceptor properties and could electrochemically bind both small donor molecules and bulk macrocyclic compounds.[25,26] In addition, the high-volume molecules caused redox-switchable self-assembly of these VRs.

Herein, we constructed water-soluble nanoparticles through self-assembly of VR cavitands. The presence of eight positive charges on the upper ri^m, alkyl chains on the lower rim, and

[a] Dr. R. R. Kashapov, Dr. S. V. Kharlamov, E. D. Sultanova, R. K. Mukhitova, Dr. Y. R. Kudryashova, Prof. Dr. L. Y. Zakharova, Dr. A. Y. Ziganshina, Prof. Dr. A. I. Konovalov
A.E. Arbuzov Institute of Organic and Physical Chemistry
Kazan Scientific Center, Russian Academy of Sciences
Arbuzov Str. 8, 420088 Kazan (Russian Federation)
Fax: (+7) 8432732253
E-mail: kashapov@iopc.ru

Supporting information for this article is available on the WWW under http://dx.doi.org/10.1002/chem.201403721.

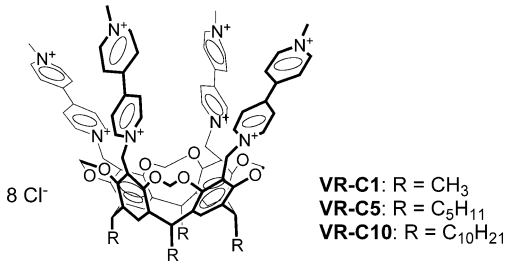

Scheme 1. Chemical structure of VR cavitands.

aromatic rings between these rims suggests that VR cavitands will exhibit amphiphilic properties and self-assemble in aqueous media. Four viologen units of a calixarene framework present the corresponding site for the counterion, the effect of which may be responsible for changing the association model of cavitands. Herein, we compare the self-assembly properties in aqueous solutions of a series of VRs with methyl (VR-C1), *n*-pentyl (VR-C5), and *n*-decyl (VR-C10) substituents on the lower rim (Scheme 1). Thus, the aim of this study was to investigate the effect of the length of the alkyl group on the lower rim and the nature of the counterion on the self-assembly behavior of VR cavitands.

Results and Discussion

Dependence of VR cavitand self-assembly on chain length

Three VRs, VR-C1, VR-C5, and VR-C10, were studied in aqueous solutions. The cavitands VR-C5 and VR-C10 show amphiphilic properties that determine their ability to self-organize. Diffusion NMR spectroscopy data indicate that increasing the concentration, *C*, of these cavitands results in a decrease in their self-diffusion coefficients, *D* (Figure 1), indicating the self-association of both VR-C5 and VR-C10 with critical association concentration (CAC) values of 3 and 0.3 mM, respectively. For cavitand VR-C1 with short methyl groups on the lower rim, the decrease of *D* was not observed up to 15 mM. The difference in behavior with respect to VR-C5 and VR-C10 might be due to the short length of the VR-C1 alkyl chains, the hydrophobicity of which is insufficient to drive them away from water.

Self-assembly of the studied resorcinarenes was confirmed by conductometric measurements (Figure S1 in the Supporting Information). The CAC values obtained by this method are in good agreement with NMR spectroscopy diffusion experiments and were found to be about 5 and 0.25 mM for VR-C5 and VR-C10, respectively.

To detect the hydrophobic interior of macrocycle assemblies, the solubilization of hydrophobic dye Orange OT was carried out. Assemblies formed by the cavitands studied (VR-C5, VR-C10) have a hydrophobic core region that can incorporate the dye molecules. Solubilization plots reveal that the amount of dye solubilized was low up to the CAC of each cavitand, and thereafter a sudden and steep rise was observed with the formation of assemblies in the bulk solution (Figure 2). This proves that the dye-binding process takes place in the hydrophobic site of the alkyl chains, and there is no dye interaction with viologen fragments of the upper rim. The CAC values for both cavitands obtained by this method are in good agreement with those determined by NMR spectroscopy and conductivity methods (Table S1 in the Supporting Information).

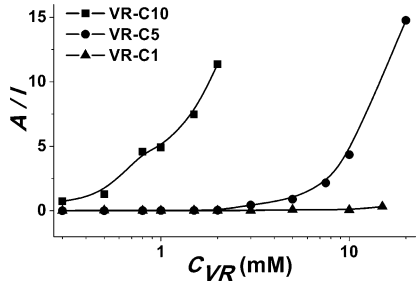

Figure 2. Changes in the Orange OT absorbance at $\lambda = 495$ nm with increasing concentration of VR cavitands (H_2O, 25 °C; $l = 0.1$ cm cell).

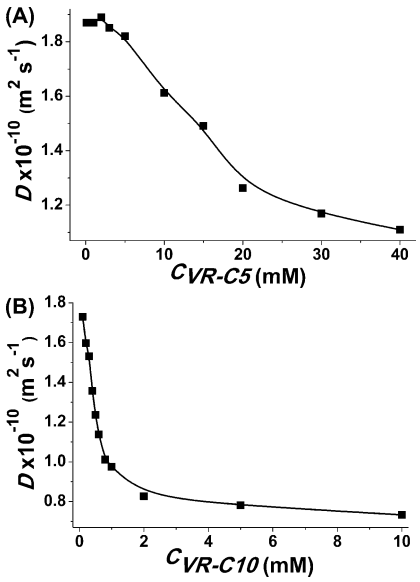

Figure 1. Concentration dependence of the self-diffusion coefficient in solutions of VR-C5 (A) and VR-C10 (B) in D_2O at 25 °C.

Less-hydrophobic VR-C1 does not dissolve the dye throughout the whole studied concentration range. This behavior is consistent with the structure of VR-C1: the short tails and charge repulsion between four bipyridinium units should prevent the formation of assemblies with hydrophobic interiors that can be loaded with hydrophobic Orange OT.

Self-association properties of cavitands could be explained by the contribution of the hydrophobic effect and electrostatic repulsion, for which the balance is determined by the length of hydrocarbon tails. As a result, the pentyl and decyl alkyl chains of VR cavitands maintain a higher level of solubilization capacity above the CAC. The obtained solubilization data for VR-C5 and VR-C10 make them an ideal choice for use as nanocontainers for hydrophobic drugs.

Although the exact shape of VR-C10 associates has not yet been resolved, the most likely shape is that of a sphere, which would display considerable anisotropy in its organization.[27] A comprehensive description of any change in organization and dynamics of such an organized assembly should include information from probes that are localized in the deeper hydrophobic core region of the associates. We therefore used a fluorescent probe, 1,6-diphenyl-l,3,5-hexatriene (DPH), to characterize the changes occurring in these regions.

The DPH molecule is oriented in the hydrophobic core of the bilayer, and thus, serves as an excellent probe for studying the order of vesicle bilayers. A unique advantage of DPH fluorescence is that, unlike some other methods, this approach is reliable even for charged detergents. This is in contrast to methods that employ charged fluorescent probes for which it has been demonstrated that such assays usually do not work if the probe and detergent have opposite charges.[28]

Fluorescence anisotropy versus concentration curves (Figure 3) showed an increase of the anisotropy value with increasing concentration of VR-C10, which suggested that the rotational mobility of DPH was considerably reduced in the cavitand associates. The increase of the anisotropy to a steady value of approximately 0.20 was observed after 1 mM VR-C10; this indicated that vesicles were probably formed.

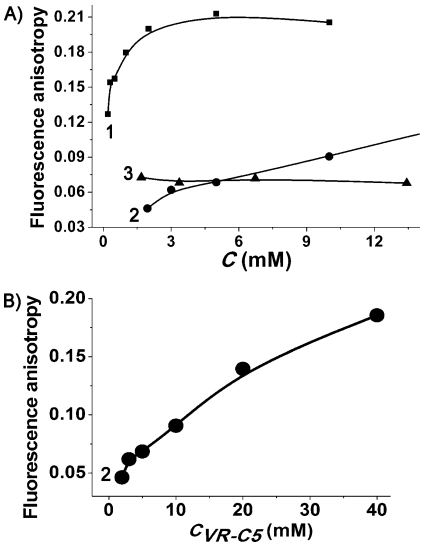

Figure 3. A) Fluorescence anisotropy of DPH complexed with VR-C10 (1), VR-C5 (2) (initial concentration range), and VR-C1 (3) in DMF/water (1:99) at 25 °C. B) The whole concentration range for VR-C5 (2).

The fluorescence experiment was also carried out with VR-C1 and VR-C5 (Figure 3). The anisotropy of DPH in a solution of VR-C1 remains more or less the same at a level of about 0.075 throughout the whole concentration range. As seen from the very low anisotropy of DPH in the VR-C1 environment, this cavitand did not form assemblies with hydrophobic interiors that could be loaded with hydrophobic DPH. The anisotropy values of VR-C5 measured at the CAC and above were lower than that of VR-C10. In this case, a smaller value of anisotropy indicates a lower degree of depolarization, and therefore, a less viscous environment.

It is possible that, if the alkyl chains on the lower rim of the cavitand are shorter and the surface charge on the upper rim is the same, another type of self-assembly could occur. Indeed, the anisotropy does not reach a plateau in the case of VR-C5 (Figure 3, inset) at concentrations above its CAC, as expected for spherical-type particles. It is a justifiable assumption that in these studies the lack of an anisotropy plateau was attributed to the head-to-tail packing direction in a higher concentration range. The size of the VR-C5 assemblies increases with increasing the molar concentration of the cavitand and, as a consequence, the anisotropy values. In addition, for aqueous solutions of calix[4]resorcinarenes and resorcin[4]arene cavitands with pentyl substituents on the lower rim,[29,30] the head-to-tail packing mode was demonstrated previously, this resulted from the cooperative contribution of weak van der Waals interactions and the hydrophobic effect. It is possible that the self-assembly behavior of VR-C5 is similar to that seen herein. Thus, the pentyl chains on the VR lower rim result in the formation of assemblies of another type than in the case of decyl chains.

In aqueous solutions, the DPH probe, when mixed with VR cavitands, gives a very pronounced bathochromic shift. An example of this shift for VR-C5 is given in Figure 4. A redshifted absorption band, which is characteristic for a ground-state charge-transfer complex formed between DPH and VR cavitand, is observed. The viologen cations mainly act as Lewis acids in solution, whereas DPH primarily exhibits Lewis base properties. These stacking interactions between DPH and VR cavitands are probably responsible for the batho- and hyperchromic shifts. Moreover, an increase in the Stokes shift is a result of the corresponding change in the microenvironment of the fluorophore with complex formation.[31] Thus, the large batho- and hyperchromic spectral changes observed in a mixed DPH–VR system are the result of strong charge-transfer chelation interactions.

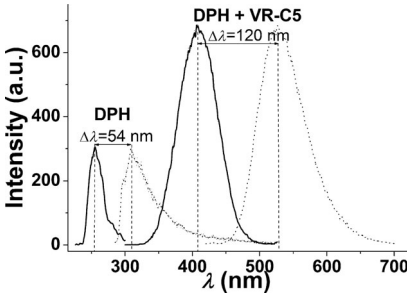

Figure 4. Excitation (continuous line) and fluorescence spectra (dotted line) of DPH in water ($\lambda_{ex}=255$ nm, $\lambda_{em}=311$ nm) and in the presence of a 1.34 mM aqueous solution of VR-C5 ($\lambda_{ex}=412$ nm, $\lambda_{em}=531$ nm), in a 1 cm cell, at 25 °C.

The hydrodynamic diameters of VR-C5 assemblies in water were 2–4 and 270–300 nm, according to dynamic light scattering (DLS) measurements (Figure S2 in the Supporting Information); this suggested that VR-C5 molecules were organized in

a manner with head-to-tail orientation and morphology. The mean size of VR-C10 assemblies ranged from 25 to 60 nm with a positive zeta potential of +34 mV (Figure S3 in the Supporting Information). These spherical particles observed by DLS probably corresponded to stable multilamellar vesicles. In addition, the anisotropy value of VR-C10 assemblies is close to 0.2, which corresponds to the bilayer structure.[32] Analysis of the self-diffusion of VR-C10 assemblies gives a hydrodynamic diameter of 5.6 nm, whereas the full length of VR-C10 is about 2.2 nm. Naturally, sphere-shaped colloidal particles with diameters much higher than the molecular dimension may be vesicular structures. The results from diffusion NMR spectroscopy and DLS methods have firmly established that VR-C10 assemblies are on the nanometer scale. In addition, one can assume that the coexistence of vesicles and elongated micelles probably occurs, which is in line with the lower value of fluorescence anisotropy within the low concentration range. We emphasize the strong complementarity of the results that ultimately lead to a better understanding of self-assembly.

Thus, after summarizing the overall results from diffusion NMR spectroscopy, conductometric, fluorescence, DLS, and solubilization experiments, the formation of multilayer spherical vesicle-like structures is more favored for VR-C10, whereas the head-to-tail packing mode takes place in the case of less-lipophilic VR-C5. No self-assembly was observed for lyophobic VR-C1.

Effect of counterions on VR cavitand self-assembly

The high charge density on the upper rim of the VR cavitands studied and the electron-acceptor properties of viologen groups suggest a significant impact of counterions on the cavitand self-assembly behavior. Multicharged assembled VR cavitands produce a strong ionic field that attracts counterions. We considered the effect of counterions of different lipophilicity and size: chloride, iodide, and benzoate ions. As it is known, iodide ions not only form an ion pair with viologens, but also interact for the formation of charge-transfer complex. Moreover, iodide ions significantly influence the electrochemical and adsorption properties of the viologen molecules. Thus, replacing chloride ions, which determined the cavitand self-assembly behavior discussed above, could lead to morphology transformation of ensembles found.

Our study shows that the iodide ions have a considerable effect on self-association of VR cavitands. In the case of VR with an iodide counterion, VR-C10-I, significant changes in conductivity and NMR spectroscopy diffusion coefficients were not found. The concentration dependence of self-diffusion coefficients and electrical conductivity of freshly prepared solutions of VR-C10-I have the same form as that of the chlorine analogue of VR-C10. However, after prolonged storage (more than 24 h) of a solution of VR-C10-I with a concentration of 0.2 mM, spectral broadening of the signals was observed. In this case, the *D* value decreases and nicely corresponds with the *D* value of an assembled cavitand (0.85×10^{-10} m^2s^{-1}).

The addition of excess potassium iodide to an aqueous solution of VR-C5 with a concentration below the CAC (0.5 mM) also causes a broadening of the proton resonance signals in the NMR spectrum. Simultaneously, the self-diffusion coefficient of VR-C5 significantly reduced to the value observed previously for assembled samples (from 1.92 to 0.97×10^{-10} m^2s^{-1}). Thus, the addition of iodide ions leads to a marked decrease in the CAC value of VR-C5.

Therefore, the self-assembly of VR cavitands in the presence of iodide ions is a thermodynamically controlled process that requires an excess amount of iodide ions or a long time for its conduction. The obtained result is mainly caused by increased ionic strength that can effectively reduce the electrostatic repulsion among the head groups of cavitands and then facilitate aggregate formation.

Generally, the effective range of electrostatic interactions of VR cavitands should be decreased with increasing electrolyte ion size. To test this, we investigated the effect of larger species, such as the benzoate ion. The introduction of various aromatic anions could modify the physicochemical properties of the assemblies in aqueous solutions.[33] In our study, the addition of benzoic acid (BA) also leads to increased self-assembly. The negatively charged BA groups are able to interact electrostatically with the VR cavitand as a counterion and undergo charge-transfer complexation with viologen fragments.

^{1}H NMR spectroscopy was applied to reveal the intermolecular interactions between BA and VR cavitands in the monomeric form. The shift of BA signals is dependent on the chain length of the VR lower rim. The presence of VR-C1 and VR-C5 species slightly affects the BA signal (Figure 5). In contrast, the addition of an equimolar amount of VR-C10 to a solution of BA resulted in a significant broadening of the BA proton signals and their upfield shift by 0.5, 0.6, and 0.95 ppm for *ortho*-, *meta*- and *para*-protons, respectively; this suggests the formation of inclusion complex species in the solution phase. In this case, the chemical shift movements are more significant than those in the presence of VR-C1 and VR-C5, revealing that the interaction between VR-C10 and BA is much stronger. The main difference is that the π–π stacking interactions of aromatic anions with aromatic viologen units are stronger due to the presence of the longer chain, which accounts for the hy-

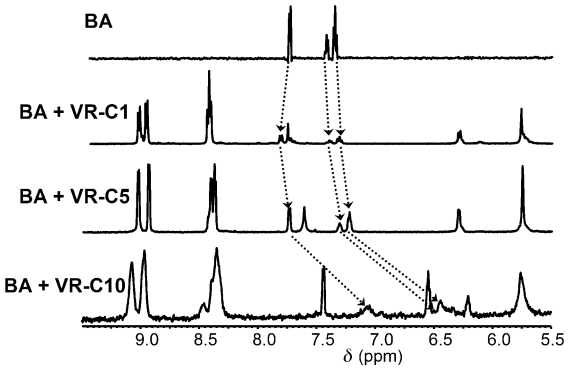

Figure 5. ^{1}H NMR spectrum (fragment) of BA in the absence and presence of equimolar amounts of VR-C*n* cavitands (*n* = 1 (1 mM), 5 (1 mM), 10 (0.2 mM)) in D_2O at 25 °C.

drophobic nature of VR-C10. This unexpected result indicates that the anions of BA may be strongly bound to the head groups of VR with more hydrophobic residues.

The Job's plot analysis shows 1:2 and 1:1 stoichiometries between VR-C10 and BA (Figure S4 in the Supporting Information). The plot for 1:2 stoichiometry is more triangular in shape, which is characteristic for stable complexes. To understand the influence of BA on association of cavitands with different lengths of alkyl tails, the molar ratios between BA and cavitands were analyzed before and after the CAC of the cavitand (Figure 6). These results showed that the shielding of the

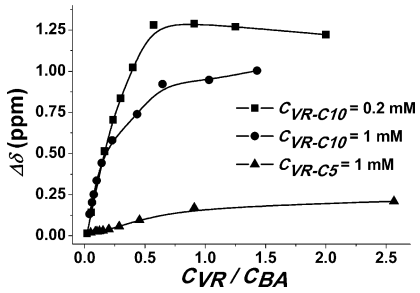

Figure 6. VR/BA concentration ratio dependence of the *para*-proton chemical shift of BA (D_2O, 25 °C).

BA molecule was greater in VR-C10 than in VR-C5. Moreover, from the slope of the titration curves, it can be concluded that BA is more tightly bound by molecules of VR-C10 than by VR-C5. Interestingly, stronger changes in the proton chemical shifts of BA in titration experiments were observed for cavitand VR-C10 before the CAC than after CAC. The BA molecules might help in the self-assembly of VR-C10, even at low concentrations of cavitand. This effect may be reflected in the highest chemical shift of BA protons in the presence of 0.2 mM VR-C10. In solution with VR-C10 assemblies, the fraction of binding sites occupied by more than one guest molecule significantly increases. Shielding of the BA protons in this respect was considered to be less pronounced. Apparently, the BA molecules are located on the surface of assemblies and are not included as deeply into the cavitand cavity as they are in the concentration range up to CAC.

A more accurate picture of the interaction of cavitands with BA was obtained from NMR diffusivity data. In the system with a concentration of VR-C10 of 1 mM, the increase in the BA concentration leads to a slight decrease in the *D* value of the cavitand (from 0.95 to 0.86×10^{-10} m^2s^{-1}; Figure 7A) and a marked increase in *D* of BA (from 2.03 to 2.32×10^{-10} m^2s^{-1}; Figure 7B). This proves the formation of host–guest complexes in solution that have lower *D* values. An increase in the *D* value of BA originates from the fact that the molar fraction of the fast component (unbinding BA) increases with the addition of BA.

An interesting pattern was observed in the titration of free non-assembled VR-C10 ($C=0.2$ mM) by BA. An increase in the BA concentration to 2 mM causes a sharp drop in the *D* value of the macrocycle down to the value that refers to the assembled form (Figure 7A). A further increase in BA concentration

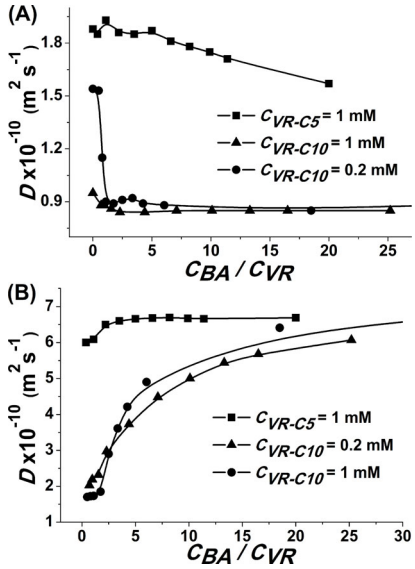

Figure 7. Dependence of the self-diffusion coefficients of VR-C5 and VR-C10 cavitands (A) and BA (B) on the VR/BA concentration ratio at a fixed cavitand concentration and varying concentrations of BA (D_2O, 25 °C).

barely changes the *D* value of VR-C10. Thus, similar to the iodide ions, BA stimulates the self-assembly of VR-C10. However, unlike the iodide ion, in this case, an equimolar amount of BA would be sufficient to shift the equilibrium towards the assembled structures of VR-C10. Importantly, in the BA concentration range of 0 to 0.4 mM, its *D* value is equal to that in a single solution of assembled cavitands (Figure 7B). In this range, BA is almost completely bound by VR-C10 binding sites. A further increase in BA concentration is accompanied with the rise of the apparent *D*, which reflects the increase in the molarity of free unbound BA molecules.

The same pattern was observed for the mixed VR-C5-BA system (Figure 7A). In this case, a 1 mM solution most likely represents free nonassembled VR-C5, and the addition to it of BA molecules leads to a gradual decrease in the *D* value of the cavitand. However, a significant proportion of assembled forms of VR-C5 was only obtained with a large excess of BA. It is important to note that even at low relative amounts of BA in a mixed solution the *D* of BA is only slightly lower than that in the individual BA solution. This proves that the degree of binding of benzoate ions by cavitand VR-C5 is relatively small.

Notably, an increase in the length of the hydrophobic tail at the lower rim of resorcin[4]arene cavitands enhances the binding of BA. A probable cause of such a different binding strength of BA is a different arrangement of VR amphiphiles during self-assembly. If the head-to-tail association is characteristic for VR-C5 and layers with alternating upper and lower rims in neighboring molecules take place, then its upper cationic rim weakly binds BA. Stronger hydrophobic interactions at the lower rim of VR-C10 drive the alkyl chains in ordered packing, whereas the viologen groups have more freedom to bind BA. Thus, the effect of the hydrophobicity of VR alkyl chains on binding to hydrophobic BA suggests that BA has a greater binding affinity to more hydrophobic VR-C10.

The trend in CAC variation for an aqueous solution of VR cavitands upon the addition of BA is similar to that in the presence of iodide ions. One possible reason for the similar behavior is that they affect the association of VR in the same way as the anions are adsorbed at the associate surface. However, the addition of BA reduces the CAC value of VR-C10 to a greater degree than iodide ions, that is, the introduction of a benzene ring makes it more effective to promote the association of VR. Electrostatic repulsion among the head groups of VR can be significantly reduced due to electrostatic attraction and π–π stacking interactions between BA and VR. Hence, an anion with phenyl rings is more efficient to promote VR self-assembly in aqueous solutions. This is mainly because the hydrophobicity of the anion is enhanced by the presence of the phenyl ring. As a result, BA is more likely to lead to stronger intermolecular interactions.

From the above results, it can be found that the aromaticity of counterions plays an important role in the assembly behavior of VR cavitands. The proposed schematic illustration of VR association change is shown in Scheme 2. This outline summarizes 1) the differences in morphological behavior for amphiphilic cavitands of different hydrophobicity; and 2) counterion-induced self-assembly of VRs. In particular, the head-to-tail association model is shown to occur for the less-hydrophobic pentyl derivative, whereas vesicles seemed to be formed in the VR-C10 system. Meanwhile, no aggregation is observed in the case of VR-C1. These assumptions are supported by the different changes in the anisotropy parameter with cavitand concentration, the size of assemblies, and the dye solubilization capacity of VRs studied. The onset of self-assembly may be controlled by the nature of counterions. For inorganic anions (i.e., iodide ions), the main interaction is their adsorption at the electrical double layer, which reduces electrostatic interactions among the VR head groups, and then macrocycle self-assembly is facilitated. The anion with an aromatic π-system may endow an additional π–π stacking interaction with cavitand. Both π–π stacking interactions and electrostatic attraction can contribute to the synergic effect between BA and VR. Owing to this relatively strong intermolecular interaction, electrostatic repulsion between VR head groups can be screened, and the association of VR is further promoted.

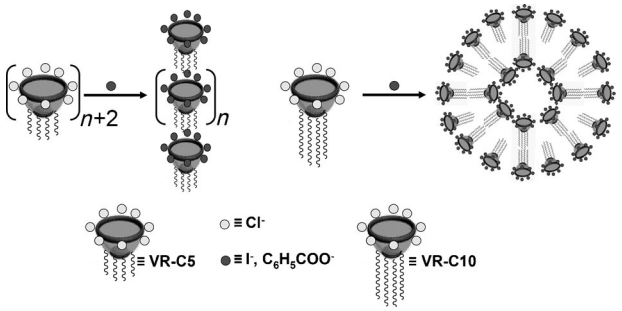

Scheme 2. Proposed schematic illustration of VR association changes in the presence of iodide and benzoate ions.

Conclusion

We investigated the association of tetraviologen resorcin[4]arene cavitands in aqueous media and showed the influence of the length of the hydrophobic tail and the nature of the counterion on their CAC. Among three structurally similar VR cavitands with a different number of methylene groups at the lower rim, different self-assembly behavior was observed. Whereas the cavitand with methyl moieties did not form assemblies, the cavitand with decyl moieties assembled into spherical aggregates. Only for the cavitand with pentyl moieties, the head-to-tail packing mode was probably observed, which was unusual for typical amphiphilic compounds. This result suggested that the length of the hydrophobic groups at the lower rim of VR cavitand controlled their self-assembly in aqueous solutions.

The replacement of the chloride counterions in VR-C5 and VR-C10 by iodide ones promoted cavitand self-assembly. Interactions of VR cavitands with benzoate resulted in a more marked increase in the assembly due to additional stabilization of the supramolecular structure. The stabilizing effect was different for similarly charged iodide and benzoate anions, which indicated that the lipophilicity and size of the counterion, along with the charge compensation effect, played determinant roles. Benzoate was more efficient at promoting the assembly of VR cavitands in aqueous solutions due to hydrophobic and π–π stacking interactions. This work is helpful in understanding the effects of anions on the self-assembly behavior of water-soluble VR cavitands and suggests that introducing an aromatic ion can effectively adjust the structure of the VR assemblies.

Experimental Section

Materials

VR-C1, VR-C5, and VR-C10 were synthesized according to a previously reported procedure.[25] Orange OT (75%, Aldrich), DPH (98%, Aldrich), potassium iodide of chemically pure grade, BA of analytically pure grade, and D_2O (99.9 atom% D, Aldrich) were used as received. Water used for the preparation of all solutions was produced by a purification system (Millipore, Direct-Q 5).

NMR spectroscopy

NMR spectroscopy experiments were performed for samples prepared in D_2O. All NMR spectroscopy experiments were performed on an Avance-600 (Bruker, Germany) spectrometer equipped with a pulsed gradient unit capable of producing magnetic field pulse gradients in the z direction of about 56 $G\,cm^{-1}$. Chemical shifts were reported relative to HDO ($\delta = 4.7$ ppm) as an internal standard. The DOSY spectra were acquired with the BPP-STE-LED pulse program. The diffusion delay was 50 ms in all cases, the bipolar gradient pulses duration was varied from 5 to 7 ms (depending on the system under investigation), 1.1 ms spoil gradient pulse (30%), and a 5 ms eddy current delay. The reported results were the mean value of multiple data points (from 2 to 6), and the standard deviations were less than 5%. All diffusion NMR spectroscopy measurements were performed at $(25 \pm 0.1)^\circ$ with a 535 $L\,h^{-1}$ air-

flow rate to avoid any temperature fluctuations owing to sample heating during the magnetic field pulse gradients.

Conductivity measurements

The conductivity was measured by using an InoLab Cond 720 conductometer (WTW GmbH, Weilheim, Germany) with a graphite electrode with a cell constant of 0.475 cm^{-1} ±1.5%. Reproducibility was checked for selected samples and no significant differences were observed. All samples were studied at 25 °C.

Orange OT solubilization

The solubilization experiments were performed by adding an excess of crystalline Orange OT dye to solutions. These solutions were allowed to equilibrate for about 48 h at room temperature. They were filtered, and their absorbency was measured at $\lambda =$ 500 nm (molar extinction coefficient 17400 $M^{-1}cm^{-1}$) on a Specord 250 Plus spectrophotometer (Analitic Jena, Germany) equipped with WinAspect software at (25 ± 0.1)° at a 0.1 cm path length cell. Absorbance of the dye for each sample was obtained by subtraction of the contribution of components to the summary spectrum. Reproducibility was checked for selected samples and no significant differences were observed.

DLS measurements and aqueous electrophoresis

DLS studies were conducted at 25 °C by using a Zetasizer Nano instrument (Malvern, UK) equipped with a 4 mW He–Ne laser operating at $\lambda = 633$ nm. Correlation data were fitted by using the method of cumulants to the logarithm of the correlation function to yield the diffusion coefficient. Backscattered light was detected at 173°, and the number-average hydrodynamic diameter was calculated by using the Stokes–Einstein equation. The diffusion coefficient was measured at least 5 times in 10 runs, so that ≥50 scans were obtained for each sample. The solutions were filtered with Millipore filters to remove dust particles from the scattering volume. Zeta-potential measurements were conducted by using the same Malvern Zetasizer Nano instrument described above. Zeta potentials were calculated from electrophoretic mobilities by using the Smoluchowski relationship. All light scattering data (DLS and aqueous electrophoresis) were processed by using Malvern Zetasizer Software.

Fluorescence measurements

Fluorescence emission spectra and steady-state anisotropy measurements were performed on a Cary Eclipse fluorescence spectrophotometer (USA). The excitation and emission slit widths were 20 and 10 nm, respectively. The embedded software automatically determined the correction factor and anisotropy value. A quartz cell of 1 cm path length was used for all fluorescence measurements. A temperature of 25 °C was maintained. VR cavitand solutions were prepared by the stepwise dilution of a stock sample. A fixed concentration of fluorescence probe DPH of 0.05 mM was used.

Acknowledgements

The work was supported by Russian Foundation for Basic Research (projects 12-03-00379, 14-03-31141). R.R.K. acknowledges a Russian Presidential Fellowship (SP-6310.2013.4).

Keywords: cavitands · hydrophobic effect · self-assembly · nanocontainers · supramolecular chemistry

[1] K. J. M. Bishop, C. E. Wilmer, S. Soh, B. A. Grzybowski, *Small* **2009**, *5*, 1600 – 1630.
[2] a) M. Ramanathan, L. K. Shrestha, T. Mori, Q. Ji, J. P. Hill, K. Ariga, *Phys. Chem. Chem. Phys.* **2013**, *15*, 10580 – 10611; b) M. Grzelczak, J. Vermant, E. M. Furst, L. M. Liz-Marza, *ACS Nano* **2010**, *7*, 3591 – 3605; c) T. G. Leong, A. M. Zarafshar, D. H. Gracias, *Small* **2010**, *6*, 792 – 806.
[3] a) R. Warmuth, J. Yoon, *Acc. Chem. Res.* **2001**, *34*, 95 – 105; b) J. Yoon, D. J. Cram, *J. Am. Chem. Soc.* **1997**, *119*, 11796 – 11806; c) D. G. Shchukin, H. Möhwald, *Chem. Commun.* **2011**, *47*, 8730 – 8739; d) J. Zhang, Y. Liu, B. Yuan, Z. Wang, M. Schönhoff, X. Zhang, *Chem. Eur. J.* **2012**, *18*, 14968 – 14973.
[4] a) J. Dormann, A. Ruoff, J. Schatz, M. O. Vysotsky, V. Bohmer, *J. Chem. Soc., Perkin Trans. 2* **2002**, 83 – 87; b) B. Breiner, J. K. Clegg, J. R. Nitschke, *Chem. Sci.* **2011**, *2*, 51 – 56; c) X. Chen, X. Ding, Z. Zheng, Y. Peng, *Macromol. Rapid Commun.* **2004**, *25*, 1575 – 1578; d) D. Ajami, J. Rebek, *Supramol. Chem.* **2013**, *25*, 574 – 580.
[5] M. Strobel, K. Kita-Tokarczyk, A. Taubert, C. Vebert, P. A. Heiney, M. Chami, W. Meier, *Adv. Funct. Mater.* **2006**, *16*, 252 – 259.
[6] M. Lee, S.-J. Lee, L.-H. Jiang, *J. Am. Chem. Soc.* **2004**, *126*, 12724 – 12725.
[7] O. M. Martin, S. Mecozzi, *Supramol. Chem.* **2005**, *17*, 9 – 15.
[8] T. N. Pashirova, E. M. Gibadullina, A. R. Burilov, R. R. Kashapov, E. P. Zhiltsova, V. V. Syakaev, W. D. Habicher, M. H. Rümmeli, S. K. Latypov, A. I. Konovalov, L. Y. Zakharova, *RSC Adv.* **2014**, *4*, 9912 – 9919.
[9] D. J. Cram, J. M. Cram in *Container Molecules and Their Guests*, (Ed.: J. F. Stoddart), Royal Society of Chemistry, Cambridge, **1997**, pp. 131-148..
[10] M. Munakata, L. Wu, T. Kuroda-Sowa, M. Maekawa, Yu. Suenaga, K. Sugimoto, I. Ino, *J. Chem. Soc. Dalton Trans.* **1999**, 373 – 378.
[11] L. R. MacGillivray, J. L. Atwood, *Nature* **1997**, *389*, 469 – 472.
[12] a) L. Avram, Y. Cohen, *J. Am. Chem. Soc.* **2002**, *124*, 15148 – 15149; b) L. Avram, Y. Cohen, *Org. Lett.* **2002**, *4*, 4365 – 4368; c) L. Avram, Y. Cohen, *Org. Lett.* **2003**, *5*, 1099 – 1102; d) L. Avram, Y. Cohen, *Org. Lett.* **2003**, *5*, 3329 – 3332; e) L. Avram, Y. Cohen, *J. Am. Chem. Soc.* **2003**, *125*, 16180 – 16181; f) L. Avram, Y. Cohen, *J. Am. Chem. Soc.* **2004**, *126*, 11556 – 11563; g) L. Avram, Y. Cohen, *J. Am. Chem. Soc.* **2005**, *127*, 5714 – 5719; h) T. Evan-Salem, Y. Cohen, *Chem. Eur. J.* **2007**, *13*, 7659 – 7663.
[13] a) A. Shivanyuk, J. Rebek, Jr., *Chem. Commun.* **2001**, 2424 – 2425; b) A. Shivanyuk, J. Rebek, Jr., *J. Am. Chem. Soc.* **2003**, *125*, 3432 – 3433; c) M. Yamanaka, A. Shivanyuk, J. Rebek, Jr., *J. Am. Chem. Soc.* **2004**, *126*, 2939 – 2943; d) E. S. Barrett, T. J. Dale, J. Rebek, Jr., *J. Am. Chem. Soc.* **2007**, *129*, 3818 – 3819.
[14] K. N. Rose, L. J. Barbour, G. W. Orr, J. L. Atwood, *Chem. Commun.* **1998**, 407 – 408.
[15] O. Ugono, K. T. Holman, *Chem. Commun.* **2006**, 2144 – 2146.
[16] K. Koh, K. Araki, S. Shinkai, *Tetrahedron Lett.* **1994**, *35*, 8255 – 8258.
[17] M. Munakata, L. P. Wu, T. Kuroda-Sowa, M. Maekawa, Y. Suenaga, K. Sugimoto, I. Ino, *J. Chem. Soc. Dalton Trans.* **1999**, *3*, 373 – 378.
[18] B. Kim, R. Balasubramanian, W. Pérez-Segarra, A. Wei, B. Decker, J. Mattay, *Supramol. Chem.* **2005**, *17*, 173 – 180.
[19] B. Peles-Lemli, J. Peles-Lemli, I. Bitter, L. Kollár, G. Nagy, S. Kunsági-Máté, *J. Inclusion Phenom. Macrocyclic Chem.* **2007**, *59*, 251 – 256.
[20] T. Haino, M. Hirakata, K. Niimi, M. Kouchi, H. Iwamoto, Y. Fukazawa, *Chem. Lett.* **2008**, *37*, 394 – 395.
[21] H. Iwamoto, K. Niimi, T. Haino, Y. Fukazawa, *Tetrahedron* **2009**, *65*, 7259 – 7267.
[22] I.-W. Park, S.-K. Kim, M.-J. Lee, V. M. Lynch, J. L. Sessler, C.-H. Lee, *Chem. Asian J.* **2011**, *6*, 2911 – 2915.
[23] a) V. G. Organo, V. Sgarlata, F. Firouzbakht, D. M. Rudkevich, *Chem. Eur. J.* **2007**, *13*, 4014 – 4023; b) H. Iwamoto, S. Nishi, T. Haino, *Chem. Commun.* **2011**, *47*, 12670 – 12672; c) J. Valero, J. De Mendoza, *Supramol. Chem.* **2013**, *25*, 728 – 740.
[24] a) U. Lucking, F. C. Tucci, D. M. Rudkevich, J. Rebek, Jr., *J. Am. Chem. Soc.* **2000**, *122*, 8880 – 8889; b) K. Rissanen, *Angew. Chem.* **2005**, *117*, 3718 – 3720; *Angew. Chem. Int. Ed.* **2005**, *44*, 3652 – 3654; c) D. E. Korshin, R. R. Kashapov, L. I. Murtazina, R. K. Mukhitova, S. V. Kharlamov, S. K. Latypov, I. S. Ryzhkina, A. Y. Ziganshina, A. I. Konovalov, *New J. Chem.* **2009**, *33*, 2397 – 2401; d) R. R. Kashapov, T. N. Pashirova, S. V. Kharlamov, A. Y. Zi-

ganshina, E. P. Ziltsova, S. S. Lukashenko, L. Y. Zakharova, W. D. Habicher, S. K. Latypov, A. I. Konovalov, *Phys. Chem. Chem. Phys.* **2011**, *13*, 15891 – 15898; e) H. D. F. Winkler, E. V. Dzyuba, J. A. W. Sklorz, N. K. Beyeh, K. Rissanen, C. A. Schalley, *Chem. Sci.* **2011**, *2*, 615 – 624; f) S. V. Kharlamov, R. R. Kashapov, T. N. Pashirova, E. P. Zhiltsova, S. S. Lukashenko, A. Y. Ziganshina, A. T. Gubaidullin, L. Y. Zakharova, M. Gruner, W. D. Habicher, A. I. Konovalov, *J. Phys. Chem. C* **2013**, *117*, 20280 – 20288.

[25] A. Y. Ziganshina, S. V. Kharlamov, D. E. Korshin, R. K. Mukhitova, E. Kh. Kazakova, S. K. Latypov, V. V. Yanilkin, A. I. Konovalov, *Tetrahedron Lett.* **2008**, *49*, 5312 – 5315.

[26] a) G. R. Nasybullina, V. V. Yanilkin, N. V. Nastapova, D. E. Korshin, A. Y. Ziganshina, A. I. Konovalov, *J. Inclusion Phenom. Macrocyclic Chem.* **2012**, *72*, 299 – 308; b) V. V. Yanilkin, G. R. Nasybullina, N. V. Nastapova, A. Y. Ziganshina, D. E. Korshin, Y. S. Spiridonova, M. Gruner, W. D. Habicher, A. A. Karasik, A. I. Konovalov, *Electrochim. Acta* **2013**, *111*, 466 – 4736; c) A. Yu. Ziganshina, G. R. Nasybullina, V. V. Yanilkin, N. V. Nastapova, D. E. Korshin, Yu. S. Spiridonova, R. R. Kashapov, M. Gruner, W. D. Habicher, A. A. Karasik, A. I. Konovalov, *Russ. J. Electrochem.* **2014**, *50*, 142 – 153.

[27] J. R. Lakowicz, *Principles of Fluorescence Spectroscopy*, 3edrd edSpringer, New York, **2006**.

[28] A. Chattopadhyay, E. London, *Anal. Biochem.* **1984**, *139*, 408 – 412.

[29] C. Aakeroy, N. Schultheiss, J. Desper, *CrystEngComm* **2007**, *9*, 211 – 214.

[30] V. V. Syakaev, A. R. Mustafina, J. G. Elistratova, S. K. Latypov, A. I. Konovalov, *Supramol. Chem.* **2008**, *20*, 453 – 460.

[31] B. Valeur, *Molecular Fluorescence: Principles and Applications*, 2ednd ed-Wiley-VCH, Weinheim, **2012**.

[32] M. A. Voronin, D. R. Gabdrakhmanov, R. N. Khaibullin, I. Y. Strobykina, V. E. Kataev, B. Z. Idiyatullin, D. A. Faizullin, Y. F. Zuev, L. Y. Zakharova, A. I. Konovalov, *J. Colloid Interface Sci.* **2013**, *405*, 125 – 133.

[33] a) V. Srinivasan, D. Blankschtein, *Langmuir* **2003**, *19*, 9946 – 9961; b) D. F. Yu, X. Huang, M. L. Deng, Y. Y. Lin, L. X. Jiang, J. B. Huang, Y. L. Wang, *J. Phys. Chem. B* **2010**, *114*, 14955 – 14964; c) Y. Gu, L. Shi, X. Cheng, F. Lu, L. Zheng, *Langmuir* **2013**, *29*, 6213 – 6220.

Received: May 28, 2014
Published online on September 10, 2014